Published OnlineFirst December 13, 2011; DOI: 10.1158/0008-5472.CAN-11-2584

A Pharmacologic Inhibitor of the Protease Taspase1 Effectively Inhibits Breast and Brain Tumor Growth

David Y. Chen[1], Yishan Lee[1], Brian A. Van Tine[1], Adam C. Searleman[1], Todd D. Westergard[1], Han Liu[3], Ho-Chou Tu[3], Shugaku Takeda[3], Yiyu Dong[3], David R. Piwnica-Worms[2], Kyoung J. Oh[6], Stanley J. Korsmeyer[7†], Ann Hermone[8], Richard Gussio[8], Robert H. Shoemaker[9], Emily H.-Y. Cheng[3,4], and James J.-D. Hsieh[3,5]

Abstract

The threonine endopeptidase Taspase1 has a critical role in cancer cell proliferation and apoptosis. In this study, we developed and evaluated small molecule inhibitors of Taspase1 as a new candidate class of therapeutic modalities. Genetic deletion of Taspase1 in the mouse produced no overt deficiencies, suggesting the possibility of a wide therapeutic index for use of Taspase1 inhibitors in cancers. We defined the peptidyl motifs recognized by Taspase1 and conducted a cell-based dual-fluorescent proteolytic screen of the National Cancer Institute diversity library to identify Taspase1 inhibitors (TASPIN). On the basis of secondary and tertiary screens the 4-[(4-arsonophenyl)methyl]phenyl] arsonic acid NSC48300 was determined to be the most specific active compound. Structure–activity relationship studies indicated a crucial role for the arsenic acid moiety in mediating Taspase1 inhibition. Additional fluorescence resonance energy transfer–based kinetic analysis characterized NSC48300 as a reversible, noncompetitive inhibitor of Taspase1 (K_i = 4.22 μmol/L). In the MMTV-neu mouse model of breast cancer and the U251 xenograft model of brain cancer, NSC48300 produced effective tumor growth inhibition. Our results offer an initial preclinical proof-of-concept to develop TASPINs for cancer therapy. *Cancer Res; 72(3); 736–46. ©2011 AACR.*

Introduction

Site-specific proteolysis offers spatiotemporal controls over fundamental aspects of organismal and cellular physiology (1–9). Accordingly, the identification and characterization of regulatory proteases in the context of human diseases has fueled the discovery of therapeutic interventions targeted at respective proteases (10). The best examples are the use of angiotensin-converting enzyme inhibitors, HIV protease inhibitors, and 26S proteasome inhibitors to treat hypertension, AIDS, and multiple myeloma, respectively (2, 11, 12).

Taspase1 (threonine aspartase) encodes a highly conserved 50 kDa α-β proenzyme that undergoes autoproteolysis, generating a mature α28/β22 heterodimeric protease that displays an overall α/β/β/α structure (13, 14). Taspase1 was initially purified as the protease that cleaves MLL to regulate the expression of *HOX* genes (13, 15). Subsequent studies identified additional Taspase1 substrates, including MLL2 (also known as MLL4 in the GenBank database; ref. 8), TFIIAα-β, and ALF (TFIIA like factor; ref. 16). The cloning of Taspase1 founded a novel class of endopeptidases that employs conserved amino terminal threonine of the mature β subunit to cleave peptide bonds after P1 aspartate (13).

Taspase1 is the only protease within the family of enzymes that possesses an asparaginase_2 (PF01112) homology domain, whereas other members, including L-asparaginase and glycosylasparaginase, participate in the metabolism of asparagines and the ordered breakdown of N-linked glycoproteins, respectively (13, 17). Taspase1-mediated cleavage follows a distinct aspartate residue of a conserved QXD/GXDD motif (15), suggesting that Taspase1 evolved from hydrolyzing asparagines and glycosylasparagines to cleaving polypeptides after aspartates (13). In addition to MLL, MLL2, TFIIA, and ALF, Taspase1 also proteolyzes *Drosophila* HCF (dHCF), whereas mammalian HCF is cleaved by O-GlcNAc transferase due to the loss of GXD/GXDD motif during the evolution (18, 19).

Authors' Affiliations: [1]Department of Medicine, [2]BRIGHT Institute, Molecular Imaging Center, Mallinckrodt Institute of Radiology, Washington University School of Medicine, St. Louis, Missouri; [3]Human Oncology and Pathogenesis Program, Departments of [4]Pathology and [5]Medicine, Memorial Sloan-Kettering Cancer Center, New York; [6]Department of Biochemistry and Molecular Biology, Rosalind Franklin University, The Chicago Medical School, North Chicago, Illinois; [7]Dana Farber Cancer Institute, Boston, Massachusetts; and [8]Information Technology Branch, [9]Screening Technologies Branch, Developmental Therapeutics Program, National Cancer Institute at Frederick, Frederick, Maryland

Note: Supplementary data for this article are available at Cancer Research Online (http://cancerres.aacrjournals.org/).

D.Y. Chen, Y. Lee, B.A. Van Tine, and A.C. Searleman contributed equally to this work.

†Deceased

Corresponding Author: James J.-D. Hsieh, Human Oncology and Pathogenesis Program, Memorial Sloan-Kettering Cancer Center, Z801, 415 E. 68th Street, New York, NY 10065. Phone: 646-888-3263; Fax: 646-888-3266; E-mail: hsiehj@mskcc.org

doi: 10.1158/0008-5472.CAN-11-2584

Published OnlineFirst December 13, 2011; DOI: 10.1158/0008-5472.CAN-11-2584

Initial characterization of *Taspase1*$^{-/-}$ mice discovered a critical role of Taspase1 in cell-cycle control (8). In the absence of Taspase1, cell cycle is disrupted with decreased expression of *Cyclins* and increased expression of CDK inhibitors (CDKI; ref. 8). Consequently, *Taspase1*$^{-/-}$ mouse embryonic fibroblasts (MEF) are resistant to oncogenic transformation (8). Furthermore, Taspase1 is overexpressed in primary human cancers and required for tumor maintenance in many cancer cell lines (20). Knockdown of Taspase1 disrupts proliferation in the majority of cancer cells within which a subset of cell lines also displays enhanced apoptosis (20). Of note, Taspase1 is expressed at high levels in many cancer cells (8, 21, 22) and in general increased expression positively correlates with the cellular dependence on Taspase1 (8, 20). These data suggest that Taspase1 is co-opted to promote and sustain tumorigenesis. Therefore, inhibition of Taspase1 may offer a new anticancer strategy. Here, we present our endeavors in (i) establishing the safety of Taspase1 inactivation in adult mammals using a genetically well-defined mouse model, (ii) characterizing the consensus cleavage motif of Taspase1, (iii) developing an *in vivo*, dual fluorescent, Taspase1 proteolytic screen, (iv) screening, confirming, and characterizing a small molecule TASPIN NSC48300, [4-[(4-arsonophenyl) methyl]phenyl] arsonic acid, and (v) examining the efficacy of NSC48300 in treating cancers using 2 different preclinical mouse tumor models.

Materials and Methods

Animal studies

Animal studies were approved by the Animal Studies Committee at Washington University School of Medicine. Mice carrying straight and conditional knockout alleles of Taspase1 (8), MMTV-neu (23), and MMTV-wnt (24) transgenes have been described. Tumor mass followed by bioluminescence imaging using an IVIS 100 system has been previously described (25).

Constructs, recombinant proteases, cell lines, cell culture, knockdown, and Western blot analyses

The dual fluorescent Taspase1 proteolytic reporter (DFPR) was constructed by sequentially inserting cDNA encoding enhanced green fluorescent protein (eGFP), 2XNES of MAPKK, aa 2,400 to 2,900 of hMLL, 3XNLS of SV40 large T antigen, and dsRED2 into the pMSCVpuro (Clontech) vector. Amphotropic retrovirus was produced as described (26) and utilized to infect 293T cells. The generation of recombinant Taspase1 and caspase8 has been described (13, 27). NCI60 cell lines were obtained from National Cancer Institute (NCI) Developmental Therapeutic Program (DTP). BT-474 was obtained from American Type Culture Collection. *Taspase1*$^{-/-}$ MEFs have been described (20) and were authenticated by both PCR genotyping and Western blot analysis. All of the cell lines were expanded, frozen, and used for no more than 2 months after the resuscitation of frozen aliquots. Cell culture, Taspase1 knockdown, and Western blot analyses were carried out as previously described (28).

Results

Acute deletion of Taspase1 in adult mice does not incur overt toxic phenotypes

Our *in vitro* studies using Taspase1 knockout and knockdown cells showed an important role of Taspase1 in tumor initiation and maintenance, suggesting that Taspase1 inhibitors (TASPINs) may be developed and utilized in cancer therapy (20). Because Taspase1 plays critical roles in mouse embryonic development, the application of TASPINs in children and pregnant women would be inadvisable (8). On the other hand, the few *Taspase1*$^{-/-}$ mice alive at weaning age went on to live a normal lifespan (Westergard and colleagues, unpublished data), implicating the safe use of TASPINs in adults. To evaluate whether Taspase1 can be safely inactivated in developed mammals, we induced a global deletion of the *Taspase1* gene in 7-week-old *Mx-Cre;Taspase1*$^{F/-}$ mice by administering polyinosine–polycytidine (pIpC; ref. 29). No discernible toxicities were observed in these *Taspase1*$^{-/-}$ mice (Fig. 1A–D). The efficiency of Taspase1 deletion in bone marrow, spleen, and thymus was determined (Fig. 1E). These results indicated that inactivation of Taspase1 through pharmacologic means is likely to be tolerated by adult mammals.

Critical amino acid residues within the Taspase1 cleavage consensus motif

To provide mechanistic insights about how Taspase1 recognizes its substrates, we characterized the Taspase1 cleavage motif. MLL contains 2 Taspase1 cleavage sites (CS1 and CS2) that are positioned 53 amino acids (aa) apart, among which CS2 is more conserved and more efficiently processed (Fig. 2A; refs. 13, 30). *In vitro* transcribed/translated (IVTT), ^{35}S-methionine labeled, human MLL aa 2,500 to 2,800 fragment containing a mutated CS1 site was employed as a CS2-specific cleavage reporter (p45MLL^{CS2}). Alanine scanning mutagenesis across the CS2 site (PKISQLD/GVDDG) of p45MLL^{CS2} was done and the cleavage of individual reporters by recombinant Taspase1 (rTaspase1) was examined. P1 aspartate and P1′ glycine are essential, P2 leucine, P3 glutamine, and P5 isoleucine are important, and P3′ and P4′ aspartates are dispensable (Fig. 2B). These data are consistent with the fact that P1 aspartate and P1′ glycine are absolutely conserved, P2, P3, and P5 hydrophobic residues are highly conserved, and P4 is variable, among known Taspase1 cleavage motifs (Fig. 2A). Surprisingly, highly conserved P3′ and P4′ aspartate residues are dispensable, indicating that these residues may play an indirect role in presenting substrates for Taspase1 recognition. In summary, the IXQL(V)D/G sequence represents the best Taspase1 cleavage recognition motif.

Accordingly, primitive peptidomimetic Taspase1 inhibitors, derivatives of ISQLD carrying common protease-inactivating functional groups, such as aldehyde and chloromethyl ketone (cmk), were synthesized and tested for their ability to inhibit Taspase1-mediated cleavage of p75MLL (aa 2,400–2,900). Although aldehyde and cmk are effective warheads against

Published OnlineFirst December 13, 2011; DOI: 10.1158/0008-5472.CAN-11-2584

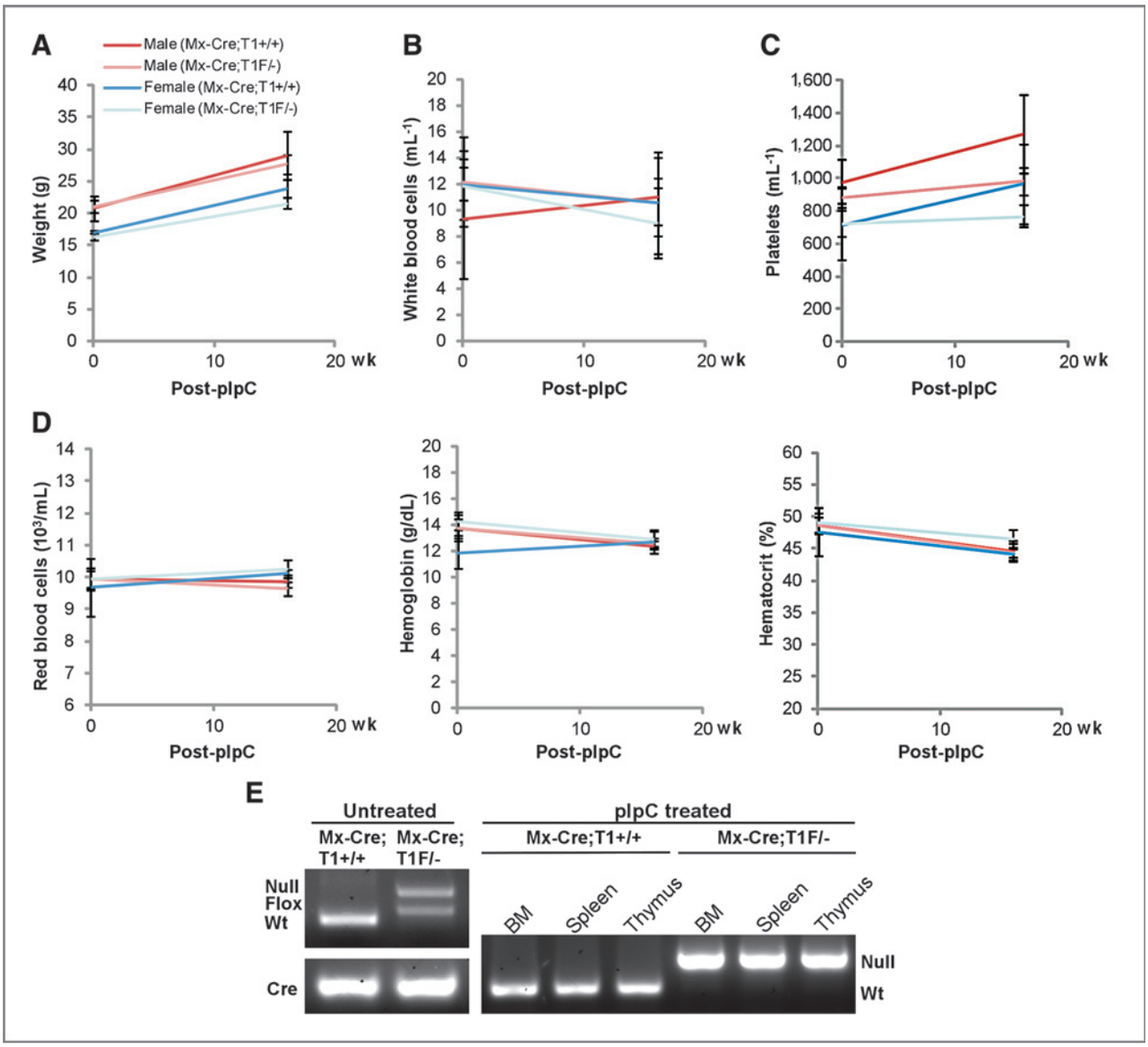

Figure 1. Induced genetic deletion of Taspase1 is well tolerated in adult mice. A, mice bearing an IFN-inducible cre recombinase (Mx-Cre) transgene and the indicated alleles of Taspase1 (+, wild type; -, knockout; F, conditional allele) at 7 weeks of age were subjected to 5 doses of pIpC injection. Baseline measurements were obtained at 6 weeks of age. Mice were sacrificed 16 weeks after the last dose of pIpC to obtain posttreatment measurements and harvest bone marrow (BM), spleen, and thymus for genotypic analysis. B–D, genetic deletion of Taspase1 does not affect the parameters of white blood cell (B), platelet (C), and red blood cell counts (D). E, genotyping of the indicated tissues shows a complete deletion of Taspase1 after the pIpC treatment.

general classes of proteases (31), ISQLD-aldehyde and ISQLD-cmk were minimally active in inhibiting Taspase1 (IC_{50} > 100 μmol/L; Supplementary Fig. S1A). Of all proteases in mammals, the β subunit of the 20S proteasome (32) is the only known N-terminal threonine endopeptidase other than Taspase1 (13). Bortezomib—a boronic acid containing chemotherapeutic drug that targets the active site threonine of the 26S proteasome (11)—has no activity against Taspase1 (Supplementary Fig. S1B), which is consistent with the lack of activity of ISQLD-boronate in inhibiting Taspase1 (33). Altogether, these data highlighted the unique mechanistic processes about Taspase1-mediated proteolysis.

A cell-based, dual-fluorescent, proteolytic screen identifies small molecule TASPINs in the NCI diversity set library

To identify bioactive, small molecule inhibitors of Taspase1, we developed an *in vivo* screen in which 293T HEK (human embryonic kidney) cells were engineered to stably express a DFPR (Fig. 3). The DFPR (eGFP-2XNES-p75MLL-3XNLS-dsRED2) consists of the CS1 and CS2 spanning human MLL polypeptide (aa 2,400–2,900, p75MLL) that is flanked by amino-terminal eGFP-NES (nuclear export signal) and carboxy terminal NLS (nuclear localization signal)-dsRED2 fusions. Taspase1-mediated cleavage of DFPR results in the

Published OnlineFirst December 13, 2011; DOI: 10.1158/0008-5472.CAN-11-2584

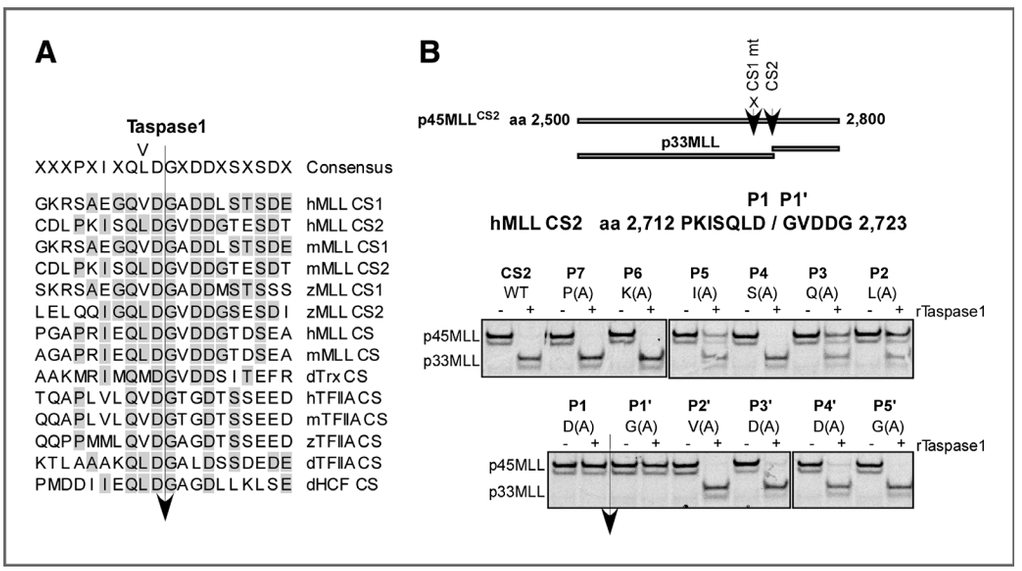

Figure 2. Characterization of the Taspase1 cleavage site consensus motif. A, alignment of known Taspase1 CS. h, m, z, and d denote human, mouse, zebra fish, and *Drosophila*, respectively. B, alanine scanning mutagenesis of the CS2 region of human MLL. The indicated p45MLL^{CS2} (aa 2,500–2,800) cleavage reporters were generated by single alanine substitution of individual amino acid across P7 to P5′ of CS2, where the CS1 was invariably mutated to enable assessment of a single cleavage site. The individual IVTT, ^{35}S-methionine labeled, p45MLL^{CS2} reporters were incubated with 15 ng of rTaspase1 (recombinant Taspase1) for 30 minutes at 30°C, resolved by SDS-PAGE and monitored by autoradiography.

distribution of green signal (eGFP/NES-p47MLL) in the cytosol and red signal (p28MLL-NLS/dsRED2) in the nucleus. Inhibition of Taspase1 would prevent cleavage of newly synthesized DFPR and result in the accumulation of yellow fluorescence. DFPR-expressing cells were screened against the NCI Diversity Set library, which identified 50 candidate inhibitors that induce varying degrees of colocalization of red–green fluorescence (Fig. 3). A secondary confirmation screen using an established Taspase1-based *in vitro* cleavage assay was carried out (13). Among candidate inhibitors, 5 showed appreciable inhibition of Taspase1-mediated cleavage of p75MLL *in vitro* (Fig. 3; Supplementary Table S1). To further characterize these small molecule TASPINs, a tertiary specificity screen was employed, in which caspase8-mediated cleavage of p22Bid was utilized to identify dual Taspase1–caspase8 inhibitors (27). Caspase8 was chosen because caspases, like Taspase1, proteolyze their substrates after P1 aspartate. The IVTT-based, caspase8-p22Bid *in vitro* cleavage assay was optimized (Supplementary Fig. S2). Interestingly, 4 of the 5 TASPINs were dual Taspase1–caspase8 inhibitors and compound #4 (NSC48300) specifically targeted Taspase1 (Fig. 3). Taken together, our cell-based screen, followed by *in vitro* confirmation and specificity assays, identified NSC48300 as a specific TASPIN.

Characteristics and structure–activity relationships of TASPIN NSC48300

The activity of TASPIN NSC48300 was evaluated using the IVTT, ^{35}S methionine-labeled p75MLL reporter, which showed an IC_{50} around 7.5 μmol/L (Fig. 4A). The mechanisms by which NSC48300 inhibits Taspase1 were further investigated. We first determined whether it effects as a reversible or irreversible inhibitor. Preincubation of Taspase1 with NSC48300 for extended periods of time did not enhance inhibition, favoring a reversible mechanism (Fig. 4B). As NSC48300 is an arsonic acid, we assessed whether free arsenic acid can inactivate Taspase1. Up to 1 mmol/L of arsenic acid was utilized and no detectable inhibition of Taspase1 was observed (Fig. 4A). Nevertheless, the arsenic acid moiety of NSC48300 seems to be essential in that its analogues NSC74084, NSC47905, NSC23953, and NSC352678, have no demonstrable activity (Fig. 4C). In addition, modifications of the benzene ring, as illustrated in arylarsonic acid NSC49855, resulted in a 10-fold decrease of the inhibitory activity (Fig. 4C). In summary, NSC48300 functions as a reversible TASPIN and arsenic acid may serve as an active functional group against Taspase1 when correctly conjugated onto appropriate chemical backbones.

Kinetic analysis of NSC48300 using a FRET-based cleavage reporter

To enable detailed kinetic analysis of TASPINs, we modified an *in vitro* FRET (fluorescence resonance energy transfer)-based Taspase1 cleavage assay (14). The FRET-based Taspase1 proteolytic reporter (FRPR, MCA-KISQLDGVDD-DNP) consists of the 10 aa CS2 consensus sequence conjugated with a fluorogenic coumarin (MCA) group and a quenching 2,4-dinitrophenyl (DNP) group at the amino and carboxy terminus, respectively (Fig. 5A). Upon Taspase1-mediated cleavage, MCA is no longer quenched by DNP, resulting in a linear increase of fluorescence emission that is excited at 328 nm and detected at 393 nm (Fig. 5B). The apparent K_M of FRPR is 9.06 ± 2.80 μmol/L (Fig. 5C). By incubating varying concentrations of FRPR and NSC48300, we showed NSC48300 as a noncompetitive TASPIN ($K_i = 4.22 \pm 0.46$ μmol/L; Fig. 5C). To confirm the noncompetitive nature of NSC48300 in inhibiting Taspase1, we employed HTI-9 (ISQLAGVDD), a weak, CS2-based, competitive peptide inhibitor of Taspase1 (Supplementary Fig. S3A

Published OnlineFirst December 13, 2011; DOI: 10.1158/0008-5472.CAN-11-2584

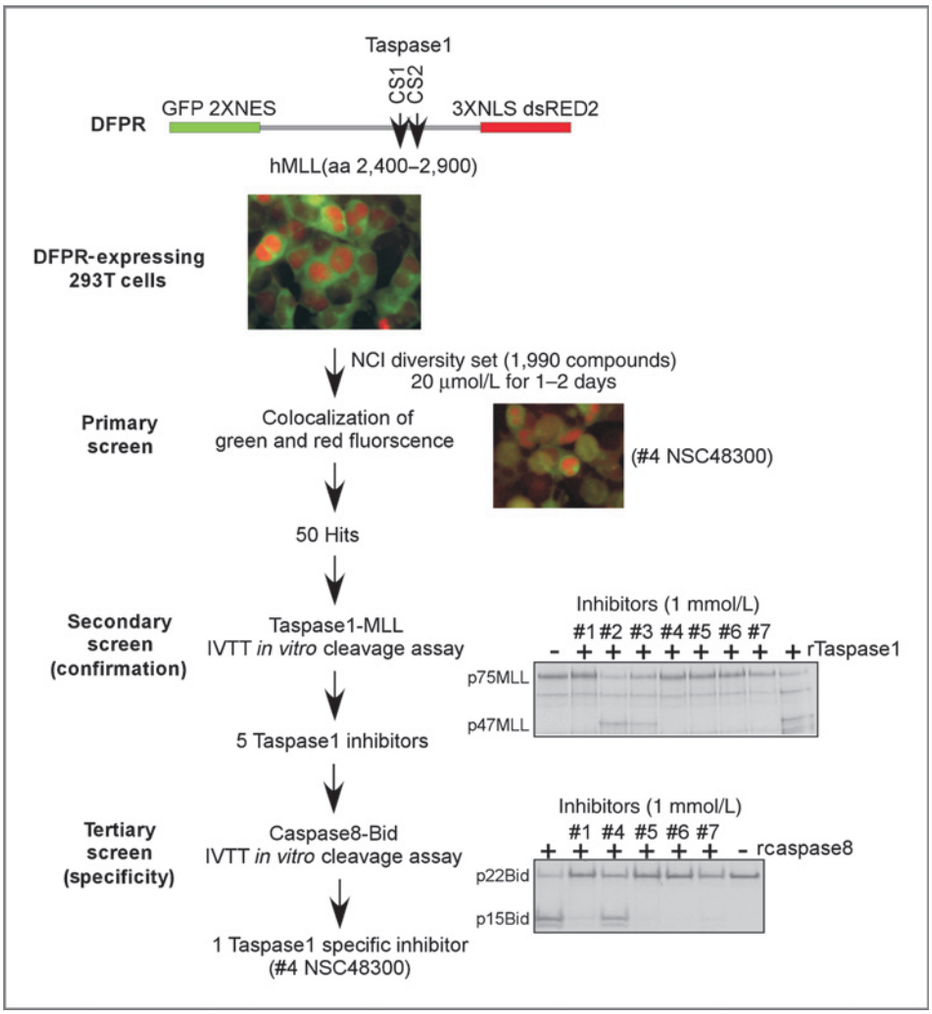

Figure 3. A novel, cell-based, DFPR identified small molecule TASPINs. Schematics depict the design of our 3-tiered screen for TASPINs. In the primary screen, DFPR expressing 293T HEK cells were treated with 20 μmol/L of the NCI DTP diversity set compounds for 2 days, and the fluorescence was determined at day 1 and 2. Pictures of DFPR expressing 293T HEK cells, either mock treated (dimethyl sulfoxide) as a negative control (top middle color picture) or compound #4 NSC48300 treated as a positive illustration (bottom right color picture), are presented. In the secondary (confirmation) screen, 15 ng of rTaspase1 was incubated with 1 mmol/L of the indicated compounds for 30 minutes before adding the radiolabeled p75MLL (aa 2,400–2,900) cleavage reporter for additional 30 minutes at 30°C. In the tertiary (specificity) screen, 250 ng of rcaspase 8 was incubated with 1 mmol/L of the indicated compounds for 30 minutes before adding the radiolabeled p22Bid cleavage reporter for 2 hours at 30°C. Cleavage was assessed by SDS-PAGE and autoradiography.

and S3B). The fact that NSC48300 and HTI-9 cooperated to inhibit Taspase1 indicates that these 2 inhibitors function at distinct sites. It confirms NSC48300 as a nonsubstrate competitive inhibitor and reveals the presence of a yet to be characterized allosteric site on Taspase1 (Fig. 5D).

NSC48300 does not inhibit the intramolecular autoproteolysis of Taspase1

Our data thus far support a working model in which NSC48300 targets an allosteric site and thereby noncompetitively inhibits Taspase1. However, it remains plausible that NSC48300 can further function by interfering the maturation step of Taspase1, that is, autoproteolysis. Taspase1 is translated as a nonprocessed α-β precursor enzyme which undergoes autoproteolysis to generate mature α/β protease (13). Taspase1 precursors can be activated by intramolecular autoproteolysis. However, whether these precursors can also be activated by mature Taspase1 through intermolecular autoproteolysis remains undetermined. To probe into the mechanism by which Taspase1 matures, radiolabeled Taspase1 precursor (p50T1α-β) was incubated in cleavage buffer alone. A slow rate of autoproteolysis with approximately 50% maturation after 6 hours of incubation was observed (Fig. 5E). If p50T1α-β can be activated by intermolecular autoproteolysis, the addition of purified rTaspase1 would greatly expedite the maturation of labeled p50T1α-β. No enhanced cleavage of p50T1α-β was observed upon the addition of up to 100 ng of rTaspase1, indicating the lack of intermolecular autoproteolysis (Supplementary Fig. S4). Altogether, Taspase1 precursors undergo intramolecular, but not intermolecular, autoproteolysis to generate mature Taspase1 enzyme. With this information in hand, increasing amounts of NSC48300 were added to the autoproteolysis reaction and no impact on the Taspase1 autoproteolysis was observed (Fig. 5F), excluding the possibility that NSC48300 inhibits Taspase1 through disrupting autoproteolysis.

The expression level of Taspase1 in breast and brain cancer cell lines correlates with sensitivity to NSC48300

With a specific TASPIN in hand, we explored its potential application in treating cancer cells. Knockdown studies using cancer cell lines showed that cells with higher expression of Taspase1 are more dependent on Taspase1 (20). Hence, we

Published OnlineFirst December 13, 2011; DOI: 10.1158/0008-5472.CAN-11-2584

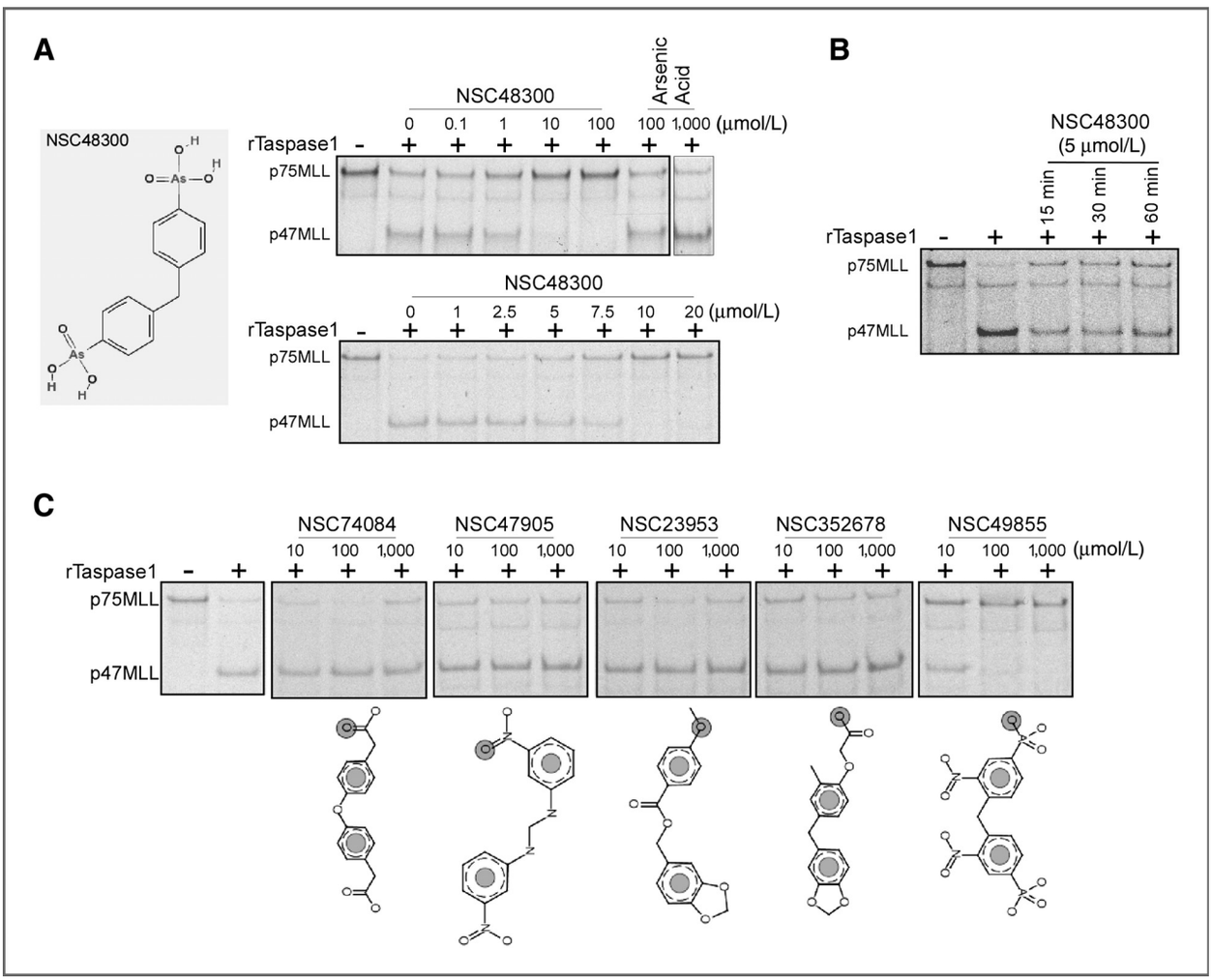

Figure 4. Characterization of NSC48300 and determination of its structure–activity relationship. A, chemical structure of NSC48300. 5 ng of rTaspase1 was incubated with the indicated concentrations of either NSC48300 or arsenic acid for 30 minutes at room temperature before adding the radiolabeled p75MLL reporter for 30 minutes at 30°C. B, five ng of rTaspase1 was incubated with 5 μmol/L of NSC48300 for the indicated periods of time at room temperature before adding the radiolabeled p75MLL reporter for 30 minutes at 30°C. C, five ng of rTaspase1 was incubated with the indicated concentrations of individual NSC48300 analogues for 30 minutes at room temperature before adding the radiolabeled p75MLL reporter for 30 minutes at 30°C. Cleavage was assessed by SDS-PAGE and autoradiography.

envisioned that certain cancer types might exhibit a strong correlation between their Taspase1 expression and sensitivity to NSC48300. To examine this hypothesis, we first employed SV40-transformed *Taspase1*$^{-/-}$ MEFs that are stably reconstituted with Taspase1 (*Taspase1*$^{-/-}$;*Taspase1*). When compared with the congenic parental *Taspase1*$^{-/-}$ cell line, *Taspase1*$^{-/-}$;*Taspase1* cells displayed increased sensitivity to NSC48300, indicating that the presence of Taspase1 renders treatment sensitivity (Fig. 6A). We next integrated the Taspase1 protein expression profile and the NSC48300 growth inhibition database of the NCI60 cancer cell lines (8, 34). According to the NCI DTP database (35), NSC48300 produces a distinct pattern of growth inhibition in the NCI60 *in vitro* anticancer drug screen (Supplementary Table S2). The sensitivity to NSC48300-mediated growth inhibition is in general agreement with the protein level of Taspase1 in many human cancer cell lines (Supplementary Table S2), among which an especially tight correlation is detected in breast and brain cancer cells (Fig. 6B and C, left panels). The differential sensitivity to NSC48300 within these 2 cancer types was confirmed (Fig. 6B and C, right panels), supporting Taspase1 as a target of NSC48300 in treating cancer cells. However, when high concentrations of NSC48300 were utilized, nonspecific toxicity became evident, which could relate to its intrinsic arsenic acid moiety or effects on other cellular enzymes. NSC48300 was recently shown to inhibit autotaxin, an extracellular enzyme that converts lysophosphatidylcholine to lipophosphatidic acid (LPA; ref. 36). The lysophospholipase D activity of autotoxin can be inhibited by NSC48300, resulting in the disruption of LPA production and a subsequent decrease of the *in vitro* invasiveness of cancer cells, which can be reversed by adding extracellular LPA (36). To examine whether

Published OnlineFirst December 13, 2011; DOI: 10.1158/0008-5472.CAN-11-2584

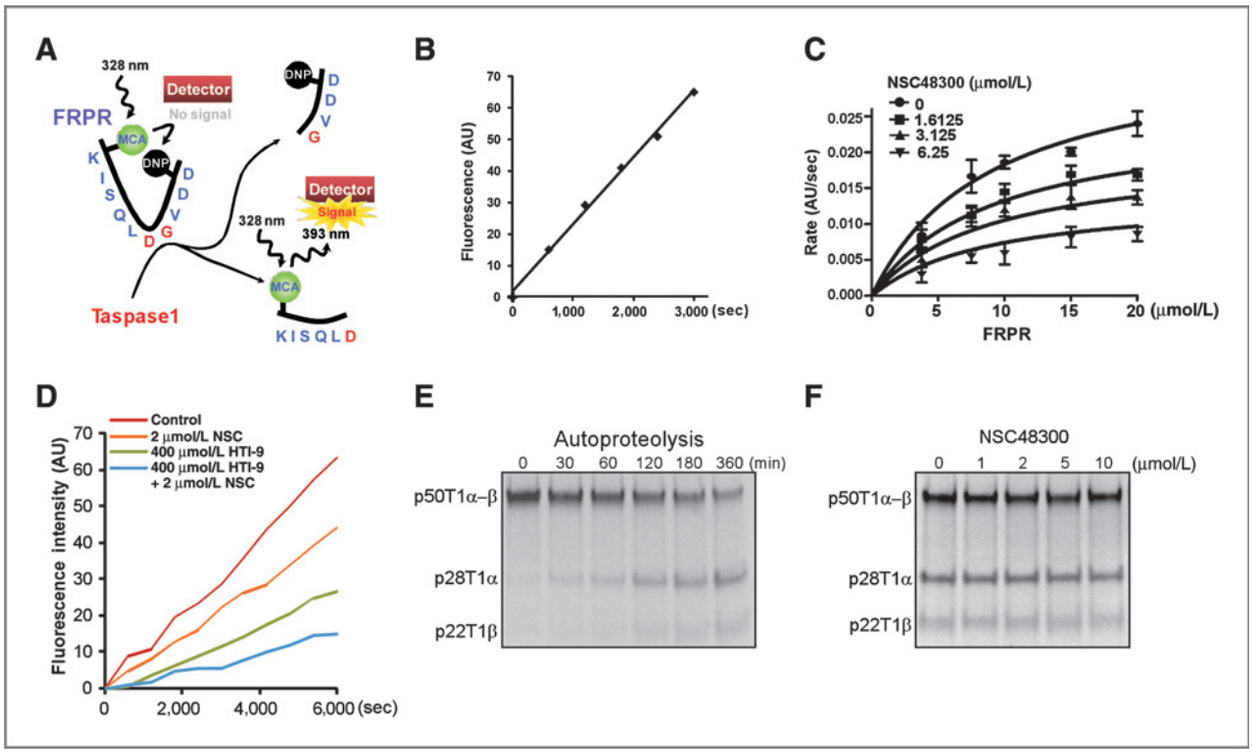

Figure 5. Enzyme kinetics analyses of NSC48300. A, diagram depicts the FRPR. B, 15 μmol/L of FRPR was incubated with 100 nmol/L of rTaspase1 and the fluorescence was monitored. AU denotes absolute fluorescence units. C, nonlinear regression of the reaction curves revealed that NSC48300 is a noncompetitive inhibitor of Taspase1. Increasing concentrations of FRPR were incubated with 100 nmol/L of rTaspase1 that was pretreated with the indicated concentrations of NSC48300. Data presented are mean ± SD of 3 independent experiments. D, hundred nmol/L of Taspase1 was preincubated for 30 minutes with the indicated concentrations of NSC48300 (NSC) and/or HTI-9 before the addition of FRPR. Reaction progress curves are shown. E, precursor Taspase1 (p50T1α-β) undergoes autoproteolysis to generate 28 kDa α (p28T1α) and 22 kDa β (p22T1β) subunits. A 0.5 μL of radiolabeled, 50 kDa precursor Taspase1 (p50T1α-β) was incubated at 30°C for the indicated periods of time. F, a 0.5 μL of radiolabeled p50T1α-β was incubated at 30°C for 6 hours in the presence of indicated concentrations of NSC48300.

our observed cancer cell sensitivity to NSC48300 can be partially attributed to the inhibition of autotaxin, we treated cancer cells with NSC48300 in the presence or absence of LPA. Because the relative cell number curves basically overlaid irrespective of LPA in both NSC48300 sensitive and insensitive lines, we excluded autotaxin as a target for NSC48300-mediated growth inhibition, which is consistent with the known extracellular expression and action of autotaxin (Fig. 6B and C, right panels).

NSC48300 inhibits the growth of MMTV-neu mouse breast cancers and U251 brain tumor xenografts

Following up on the cell line data, we wished to evaluate the *in vivo* efficacy of NSC48300 in treating cancers. Because NSC48300 is an arsonic acid and no data with regard to its *in vivo* safety have been reported, we determined its toxicity profile. Short-term, instead of long-term, tail vein injections were given due to observed fibrotic damages of regional vessels at injection sites upon repetitive treatment of NSC48300. Histologic examination of major organs did not reveal any obvious abnormalities, whereas blood chemistry revealed a significant decrease in the LDH level and certain alterations in electrolytes and kidney functions (Supplementary Fig. S5 and Table S3). Complete blood counts were also done, which showed a decrease in white blood cell counts and hemoglobin levels (Supplementary Fig. S6A–C).

To enable a scientific selection of the most relevant breast cancer model for *in vivo* experiments, we expanded our breast cancer cell line repertoire to incorporate an estrogen receptor (ER) negative, Her2/neu overexpressing cancer cell line, BT474 (37), and conducted genetic knockdown experiments (Supplementary Fig. S7). Among these 3 breast cancer cell lines, MDA-MB-231 cells, an ER negative, Her2/neu negative cell line (38) that expresses a very low level of Taspase1, were least affected by the deficiency of Taspase1 (Fig. 7A and Supplementary Fig. S7; ref. 20). By contrast, cells with higher levels of Taspase1, including MCF7, an ER positive, Her2/neu negative cell line (39), and BT-474 cells were more dependent on Taspase1 (Fig. 7A and Supplementary Fig. S7). On the basis of these *in vitro* data, Her2/neu-driven tumors may be more dependent on Taspase1 and would be more sensitive to NSC48300 treatment, whereas ER negative, Her2/neu negative breast cancers would be resistant. To examine this hypothesis *in vivo*, we treated MMTV-neu (23) or MMTV-wnt (ER-, Her2-; ref. 24) breast cancer–bearing mice with NSC48300. Indeed, NSC48300 consistently disrupted the growth of MMTV-neu breast cancers, whereas it exhibited no effects on the growth of MMTV-wnt breast cancers (Fig. 7B).

Published OnlineFirst December 13, 2011; DOI: 10.1158/0008-5472.CAN-11-2584

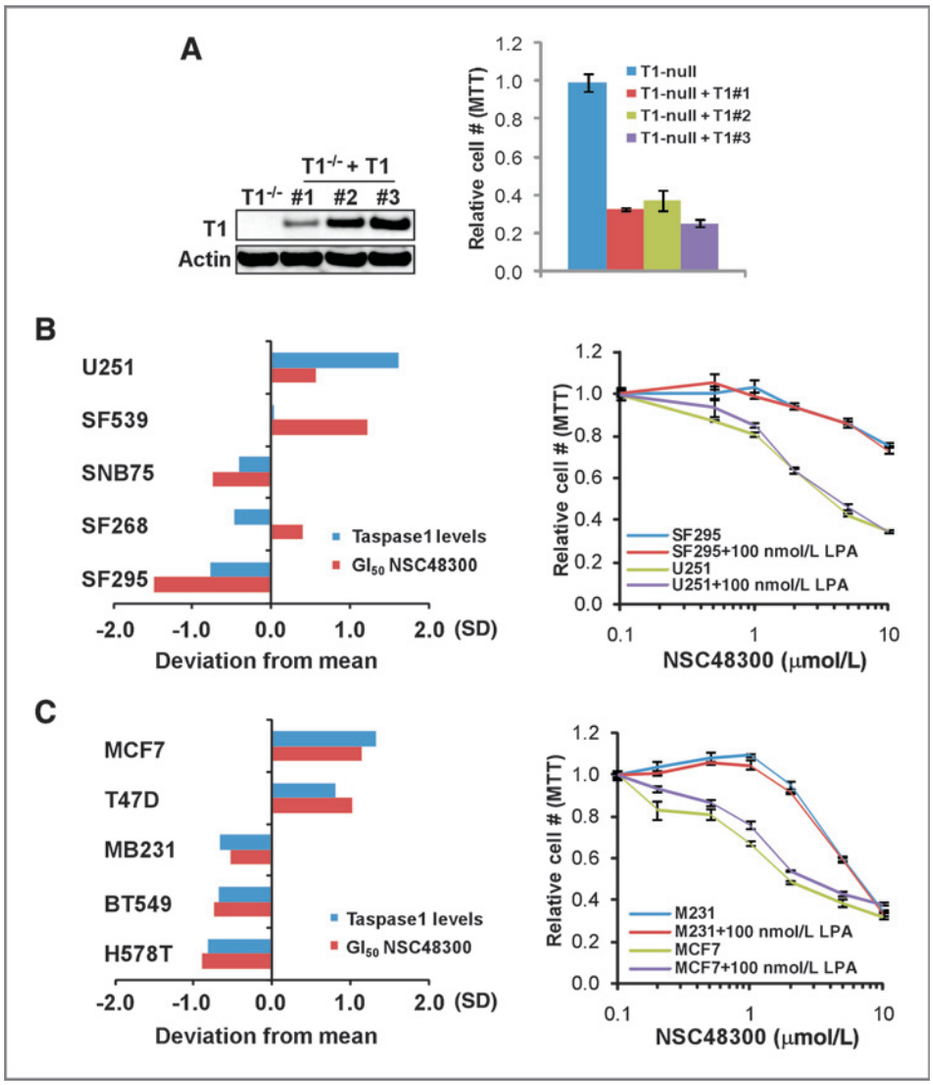

Figure 6. The cellular sensitivity to NSC48300 correlates with the protein expression of Taspase1. A, the indicated MEFs were treated with 1 μmol/L of NSC48300 for 2 days and the relative cell number was measured by MTT assays. Values obtained from the parental *Taspase1*$^{-/-}$ MEFs after NSC48300 treatment were designated as 1. Data presented are mean ± SD of 3 independent experiments. B, the NSC48300 GI_{50} (growth inhibition 50%) data were acquired through a publically available database (35). To compare relative sensitivity among different brain tumor cell lines, log (GI_{50}) values of each individual lines were obtained. The SDs of individual GI_{50} from the mean were plotted (positive values indicate higher sensitivity). The protein levels of Taspase1 in the indicated cell lines have been reported and are represented as a bar graph. The indicated brain cancer cell lines were treated with increasing concentration of NSC48300 for 2 days plus or minus 100 nmol/L LPA and then subjected to MTT assays. Data presented are mean ± SD of 2 triplicate independent experiments. C, a positive correlation of Taspase1 protein levels and cellular sensitivity to NSC48300 in the NCI60 breast tumor cell lines. Data collection, experimentations, and analyses were carried out as described in B on the indicated breast cancer cell lines.

To test the efficacy of NSC48300 in treating brain tumors, we employed a brain cancer xenograft model using U251 cells based on 2 reasons. First, knockdown of Taspase1 in U251 cells impaired cell proliferation (20). Second, among the NCI60 brain tumor cell lines, U251 cells express high levels of Taspase1 and are most sensitive to NSC48300 treatment *in vitro*. To monitor treatment response in live animals, U251 cells were first engineered to stably express firefly luciferase (fLuc) before subcutaneous implantation into mice. Bioluminescent imaging showed a stasis of tumor growth in NSC48300-treated compared with vehicle-treated tumors (Fig. 7C). In summary, our *in vivo* preclinical efficacy trials showed an antitumor effect of NSC48300 in both MMTV-neu breast cancer and U251 GBM xenograft models.

Discussion

In the evolution of cancer, individual cells must overcome a multitude of challenges and eventually exhibit hallmarks of cancer, a process demanding multiple oncogenes and non-oncogenes that function cooperatively to achieve and maintain the aberrant, oncogenic state. The evolved reliance of oncogenes on particular sets of subordinate nononcogenes during tumorigenesis, offering a novel anticancer treatment strategy aiming at tumor dependent, nononcogenes (40). Thus far, well-characterized tumor dependent, nononcogenic actors are scarce, including the 26S proteasome, HSF1 (41), and IRF4 (42), which handles the rapid protein turnover, mediates the stress response, and maintains expression of the MYC oncogene, respectively. The fact that the proteasome inhibitor bortezomib is effective against multiple myeloma in human patients substantiates this new anticancer therapeutic concept (11). Successful application of this strategy in cancer therapy relies on the identification and characterization of tumor dependent, nononcogenic factors that cancer but not normal cells heavily rely on.

Taspase1 by itself or in conjunction with MYC, RAS, or E1A fails to transform NIH/3T3 cells or primary MEFs, respectively,

Published OnlineFirst December 13, 2011; DOI: 10.1158/0008-5472.CAN-11-2584

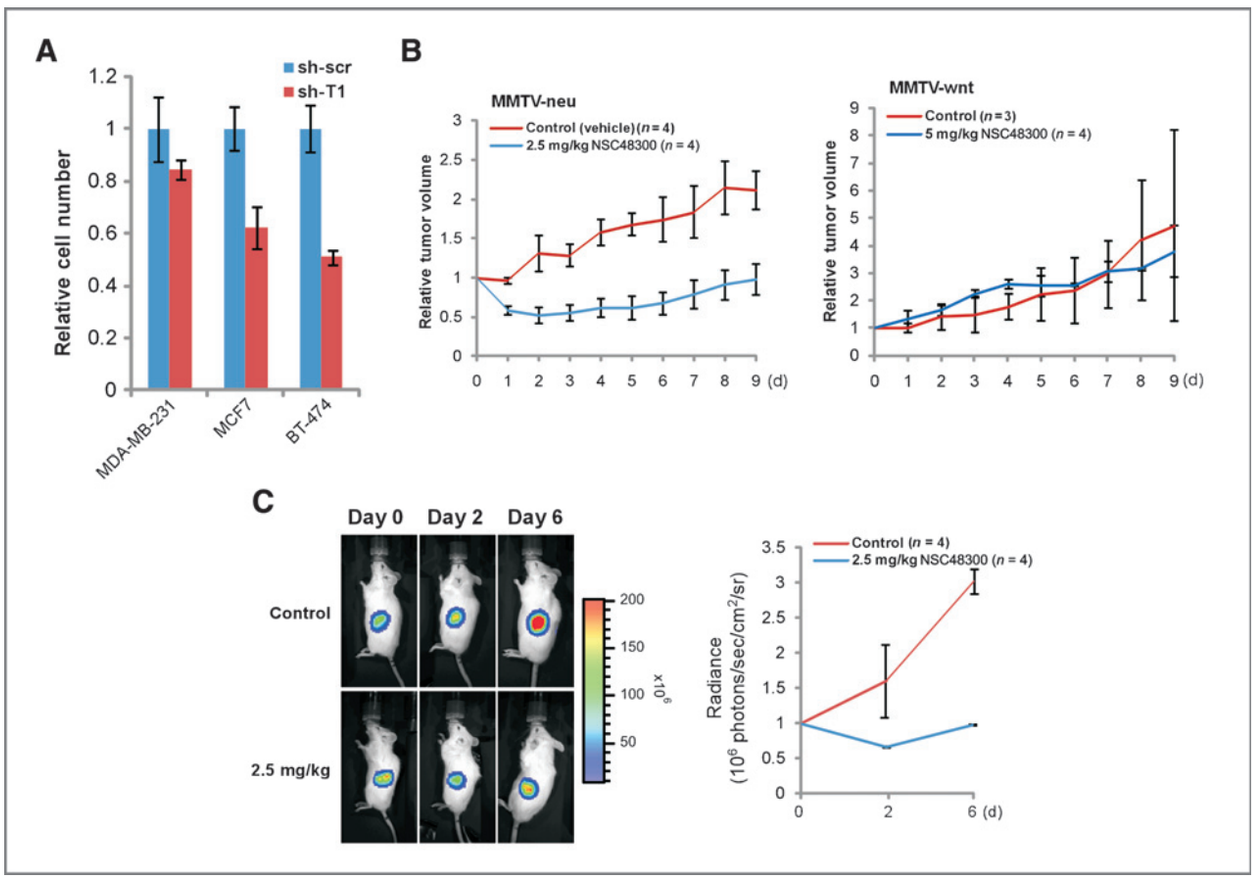

Figure 7. NSC48300 disrupts breast and brain cancer growth in mouse cancer models. A, the indicated human breast cancer cell lines with control (sh-scr) or Taspase1 (sh-T1) knockdown were plated, and cell numbers were counted 4 days after the initial plating. The average cell number of control knockdown cells was assigned as 1. Data presented are mean ± SD of 3 independent experiments. B, tumor-bearing MMTV-neu or MMTV-wnt mice were treated at day 0 when *de novo* tumors reached 1 cm at the longest dimension. NSC48300 was given at the indicated doses every other day for a total of 5 intravenous injections. Graphs represent the relative tumor volume throughout the course of treatment. The tumor size measured at day 0 immediately before treatment was assigned as 1. Data presented are mean ± SD of the indicated number of tumors of each arm. C, U251 cells transduced with a luciferase reporter were implanted into the flanks of male NOD-scid IL2Rγ$^{-/-}$ mice at 6 to 8 weeks of age (day −1). Mice were then treated on days 0, 2, and 4 with the indicated dose of NSC48300. Tumor mass was determined by bioluminescent imaging using an IVIS 100 and representative bioluminescent images are presented. The graph represents mean ± SD of 4 tumors from each arm. The absolute bioluminescence was normalized to a value of 1 at day 0.

yet is required for efficient cancer initiation and maintenance (20). Hence, Taspase1 functions as a tumor dependent, non-oncogenic protease, whose inhibition may offer an anticancer strategy. However, Taspase1 is highly conserved and known to regulate embryonic development (8). The severe perinatal lethality resulting from the embryonic loss of Taspase1 suggests that inactivation of Taspase1 by genetic or pharmacologic means is inadvisable in pregnant females and children to avoid potential developmental sequelae. In contrast, inactivation of Taspase1 in fully developed adult mammals seems to be well tolerated. Cancer commonly hijacks key developmental pathways during tumorigenesis and thus frequently exhibits unique properties, which may underlie the preferential therapeutic benefit conferred by targeting Taspase1 to treat cancers.

Through proteolytic processing of nuclear transcription regulators, Taspase1 controls cellular proliferation by suppressing and activating the expression of CDKIs and cyclins, respectively (8, 20). Although knockdown of Taspase1 affects proliferation in many cancer cell lines, candidate cancer types that may respond to Taspase1 inhibition *in vivo* remain unclear. Unlike activating mutations of epidermal growth factor receptor and BCR-ABL that can serve as powerful biomarkers for selecting responsive cancers (43), Taspase1 dose not function like a classical oncogene and is not mutated in cancers (COSMIC, Sanger Institute). Data thus far indicate a positive correlation between Taspase1 protein levels and the underlying dependence, which provides a useful primary tool in identifying potentially susceptible cancers. Our prior knockdown experiments showed an *in vitro* and *in vivo* reliance of U251 brain cancer cells on Taspase1 for a full cancer phenotype (20). Here, we show treatment response of U251 cells to TASPIN NSC48300 in both cell culture and xenograft models. Hence, genetic knockdown experiments in cancer cells could reflect the cellular dependence on Taspase1 and thus provide assessment of *in vivo* responsiveness of individual cancers to TASPINs.

Published OnlineFirst December 13, 2011; DOI: 10.1158/0008-5472.CAN-11-2584

In addition to brain tumors, we expanded our *in vivo* studies to incorporate breast cancer models. Deficiency in Taspase1 by genetic knockdown disrupts the proliferation of Her2/neu$^+$ human BT-474 breast cancer cells, suggesting that Her2-neu$^+$ breast cancer may be sensitive to the inactivation of Taspase1. Indeed, *de novo* breast cancers developed in MMTV-neu mice responded to the treatment with NSC48300, whereas MMTV-wnt breast cancers were insensitive. Consistent with the treatment effects, mammary tissue–specific knockout of Taspase1 disrupts MMTV-neu–driven, but not MMTV-wnt–driven, breast carcinogenesis (Van Tine and colleagues, unpublished data). Taspase1 seems to play an important role in the Her2/neu growth factor signaling pathway, whereas WNT signals apparently bypass Taspase1-mediated oncogenic events. These data highlight the heterogeneity underlying individual tumorigenesis and the importance of selecting the responsive cancers that may benefit from treatment with TASPINs. Further studies with regard to the involvement of Taspase1 in various oncogenic pathways and the pathogenesis of subtypes of cancers would offer a better target cancer selection for the potential use of TASPINs in the future.

Disclosure of Potential Conflicts of Interest

No potential conflicts of interests were disclosed.

Acknowledgments

The authors thank Ms. Hsiu-Fang Chen for her technical assistance and Dr. Shoemaker for editing the manuscript.

Grant Support

This study is supported by NIH CA R01-119008 and the American Cancer Society.

The costs of publication of this article were defrayed in part by the payment of page charges. This article must therefore be hereby marked *advertisement* in accordance with 18 U.S.C. Section 1734 solely to indicate this fact.

Received July 30, 2011; revised November 21, 2011; accepted December 7, 2011; published OnlineFirst December 13, 2011.

References

1. Furie B, Furie BC. Molecular and cellular biology of blood coagulation. N Engl J Med 1992;326:800–6.
2. Zaman MA, Oparil S, Calhoun DA. Drugs targeting the renin-angiotensin-aldosterone system. Nat Rev Drug Discov 2002;1:621–36.
3. Brown MS, Ye J, Rawson RB, Goldstein JL. Regulated intramembrane proteolysis: a control mechanism conserved from bacteria to humans. Cell 2000;100:391–8.
4. Ye Y, Fortini ME. Proteolysis and developmental signal transduction. Semin Cell Dev Biol 2000;11:211–21.
5. Thornberry NA, Lazebnik Y. Caspases: enemies within. Science 1998;281:1312–6.
6. Boatright KM, Salvesen GS. Mechanisms of caspase activation. Curr Opin Cell Biol 2003;15:725–31.
7. Julien E, Herr W. Proteolytic processing is necessary to separate and ensure proper cell growth and cytokinesis functions of HCF-1. EMBO J 2003;22:2360–9.
8. Takeda S, Chen DY, Westergard TD, Fisher JK, Rubens JA, Sasagawa S, et al. Proteolysis of MLL family proteins is essential for taspase1-orchestrated cell cycle progression. Genes Dev 2006;20:2397–409.
9. Saklatvala J, Nagase H, Salvesen G. Proteases and the regulation of biological processes. Biochemical Society Symposium 2002;70.
10. Docherty AJ, Crabbe T, O'Connell JP, Groom CR. Proteases as drug targets. Biochem Soc Symp 2003:147–61.
11. Adams J. The proteasome: a suitable antineoplastic target. Nat Rev Cancer 2004;4:349–60.
12. Markowitz M, Saag M, Powderly WG, Hurley AM, Hsu A, Valdes JM, et al. A preliminary study of ritonavir, an inhibitor of HIV-1 protease, to treat HIV-1 infection. N Engl J Med 1995;333:1534–9.
13. Hsieh JJ, Cheng EH, Korsmeyer SJ. Taspase1: a threonine aspartase required for cleavage of MLL and proper HOX gene expression. Cell 2003;115:293–303.
14. Khan JA, Dunn BM, Tong L. Crystal structure of human Taspase1, a crucial protease regulating the function of MLL. Structure 2005;13:1443–52.
15. Hsieh JJ, Ernst P, Erdjument-Bromage H, Tempst P, Korsmeyer SJ. Proteolytic cleavage of MLL generates a complex of N- and C-terminal fragments that confers protein stability and subnuclear localization. Mol Cell Biol 2003;23:186–94.
16. Zhou H, Spicuglia S, Hsieh JJ, Mitsiou DJ, Hoiby T, Veenstra GJ, et al. Uncleaved TFIIA is a substrate for taspase 1 and active in transcription. Mol Cell Biol 2006;26:2728–35.
17. Xu Q, Buckley D, Guan C, Guo HC. Structural insights into the mechanism of intramolecular proteolysis. Cell 1999;98:651–61.
18. Capotosti F, Hsieh JJ, Herr W. Species selectivity of mixed lineage leukemia/trithorax and HCF proteolytic maturation pathways. Mol Cell Biol 2007;27:7063–72.
19. Capotosti F, Guernier S, Lammers F, Waridel P, Cai Y, Jin J, et al. O-GlcNAc transferase catalyzes site-specific proteolysis of HCF-1. Cell 2011;144:376–88.
20. Chen DY, Liu H, Takeda S, Tu HC, Sasagawa S, Van Tine BA, et al. Taspase1 functions as a non-oncogene addiction protease that coordinates cancer cell proliferation and apoptosis. Cancer Res 2010;70:5358–67.
21. Niehof M, Borlak J. EPS15R, TASP1, and PRPF3 are novel disease candidate genes targeted by HNF4alpha splice variants in hepatocellular carcinomas. Gastroenterology 2008;134:1191–202.
22. Scrideli CA, Carlotti CG Jr, Okamoto OK, Andrade VS, Cortez MA, Motta FJ, et al. Gene expression profile analysis of primary glioblastomas and non-neoplastic brain tissue: identification of potential target genes by oligonucleotide microarray and real-time quantitative PCR. J Neurooncol 2008;88:281–91.
23. Muller WJ, Sinn E, Pattengale PK, Wallace R, Leder P. Single-step induction of mammary adenocarcinoma in transgenic mice bearing the activated c-neu oncogene. Cell 1988;54:105–15.
24. Tsukamoto AS, Grosschedl R, Guzman RC, Parslow T, Varmus HE. Expression of the int-1 gene in transgenic mice is associated with mammary gland hyperplasia and adenocarcinomas in male and female mice. Cell 1988;55:619–25.
25. Gross S, Piwnica-Worms D. Real-time imaging of ligand-induced IKK activation in intact cells and in living mice. Nat Methods 2005;2:607–14.
26. Liu H, Takeda S, Kumar R, Westergard TD, Brown EJ, Pandita TK, et al. Phosphorylation of MLL by ATR is required for execution of mammalian S-phase checkpoint. Nature 2010;467:343–6.
27. Zha J, Weiler S, Oh KJ, Wei MC, Korsmeyer SJ. Posttranslational N-myristoylation of BID as a molecular switch for targeting mitochondria and apoptosis. Science 2000;290:1761–5.
28. Ren D, Tu HC, Kim H, Wang GX, Bean GR, Takeuchi O, et al. BID, BIM, and PUMA are essential for activation of the BAX- and BAK-dependent cell death program. Science 2010;330:1390–3.
29. Kuhn R, Schwenk F, Aguet M, Rajewsky K. Inducible gene targeting in mice. Science 1995;269:1427–9.
30. Yokoyama A, Kitabayashi I, Ayton PM, Cleary ML, Ohki M. Leukemia proto-oncoprotein MLL is proteolytically processed into 2 fragments with opposite transcriptional properties. Blood 2002;100:3710–8.

Published OnlineFirst December 13, 2011; DOI: 10.1158/0008-5472.CAN-11-2584

31. Walsh CT. Enzymatic reaction mechanisms. San Francisco, California; W H Freeman & Company: 1978.
32. Coux O, Tanaka K, Goldberg AL. Structure and functions of the 20S and 26S proteasomes. Annu Rev Biochem 1996;65:801–47.
33. Lee JT, Chen DY, Yang Z, Ramos AD, Hsieh JJ, Bogyo M. Design, syntheses, and evaluation of Taspase1 inhibitors. Bioorg Med Chem Lett 2009;19:5086–90.
34. Shoemaker RH. The NCI60 human tumour cell line anticancer drug screen. Nat Rev Cancer 2006;6:813–23.
35. Developmental therapeutics program [Internet]. Bethesda (MD): The National Cancer Institute. c1990-[cited 2011 Nov 9]. Available from: http://dtp.nci.nih.gov/
36. Saunders LP, Ouellette A, Bandle R, Chang WC, Zhou H, Misra RN, et al. Identification of small-molecule inhibitors of autotaxin that inhibit melanoma cell migration and invasion. Mol Cancer Ther 2008;7:3352–62.
37. Kumar R, Shepard HM, Mendelsohn J. Regulation of phosphorylation of the c-erbB-2/HER2 gene product by a monoclonal antibody and serum growth factor(s) in human mammary carcinoma cells. Mol Cell Biol 1991;11:979–86.
38. Kang Y, Siegel PM, Shu W, Drobnjak M, Kakonen SM, Cordon-Cardo C, et al. A multigenic program mediating breast cancer metastasis to bone. Cancer Cell 2003;3:537–49.
39. Coezy E, Borgna JL, Rochefort H. Tamoxifen and metabolites in MCF7 cells: correlation between binding to estrogen receptor and inhibition of cell growth. Cancer Res 1982;42:317–23.
40. Luo J, Solimini NL, Elledge SJ. Principles of cancer therapy: oncogene and non-oncogene addiction. Cell 2009;136:823–37.
41. Dai C, Whitesell L, Rogers AB, Lindquist S. Heat shock factor 1 is a powerful multifaceted modifier of carcinogenesis. Cell 2007;130:1005–18.
42. Shaffer AL, Emre NC, Lamy L, Ngo VN, Wright G, Xiao W, et al. IRF4 addiction in multiple myeloma. Nature 2008;454:226–31.
43. Sawyers CL. The cancer biomarker problem. Nature 2008;452:548–52.

Cancer Research
The Journal of Cancer Research (1916–1930) | The American Journal of Cancer (1931–1940)

AACR American Association for Cancer Research

A Pharmacologic Inhibitor of the Protease Taspase1 Effectively Inhibits Breast and Brain Tumor Growth

David Y. Chen, Yishan Lee, Brian A. Van Tine, et al.

Cancer Res 2012;72:736-746. Published OnlineFirst December 13, 2011.